Electronic Supplementary Information (ESI)

A nickel containing polyoxometalate water oxidation catalyst

Guibo Zhu,[a] Elliot N. Glass,[a] Chongchao Zhao,[a] Hongjin Lv,[a] James W. Vickers,[a] Yurii V. Geletii,[a] Djamaladdin G. Musaev,[b] Jie Song[a] and Craig L. Hill*[a]

[a] *Department of Chemistry, Emory University, Atlanta, GA 30322*

[b] *Cherry L. Emerson Center for Scientific Computation, Emory University, Atlanta, GA 30322*

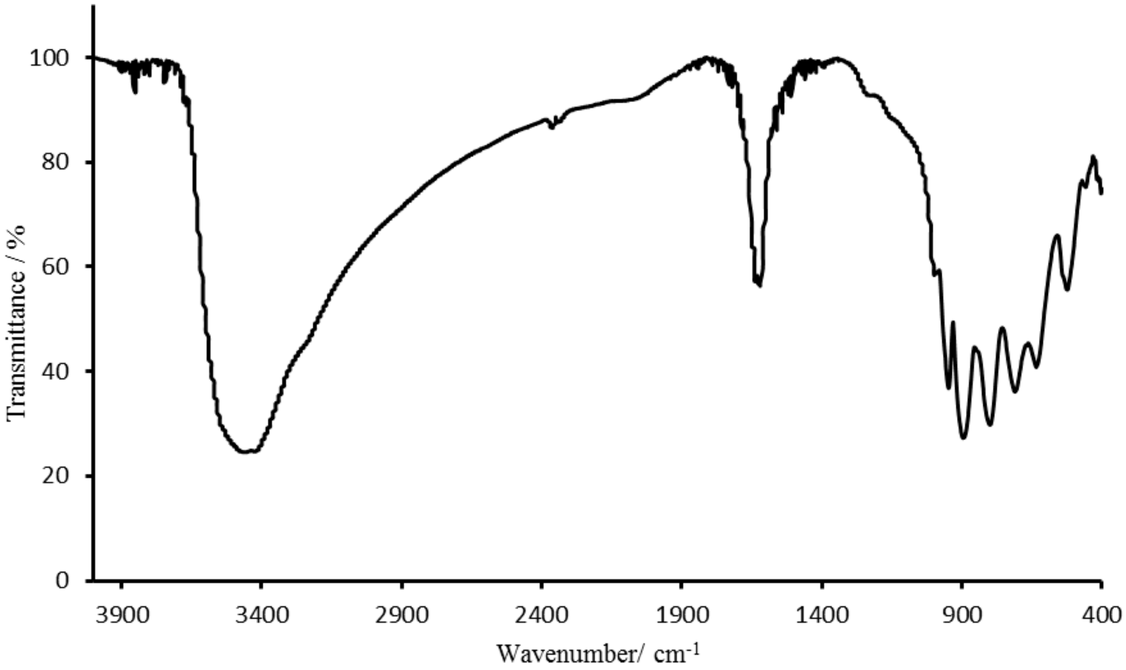

Fig. S1 Infrared spectrum of $K_{10}H_2[Ni_5(OH)_6(OH_2)_3(Si_2W_{18}O_{66})]\cdot34H_2O$ (KH-**1**).

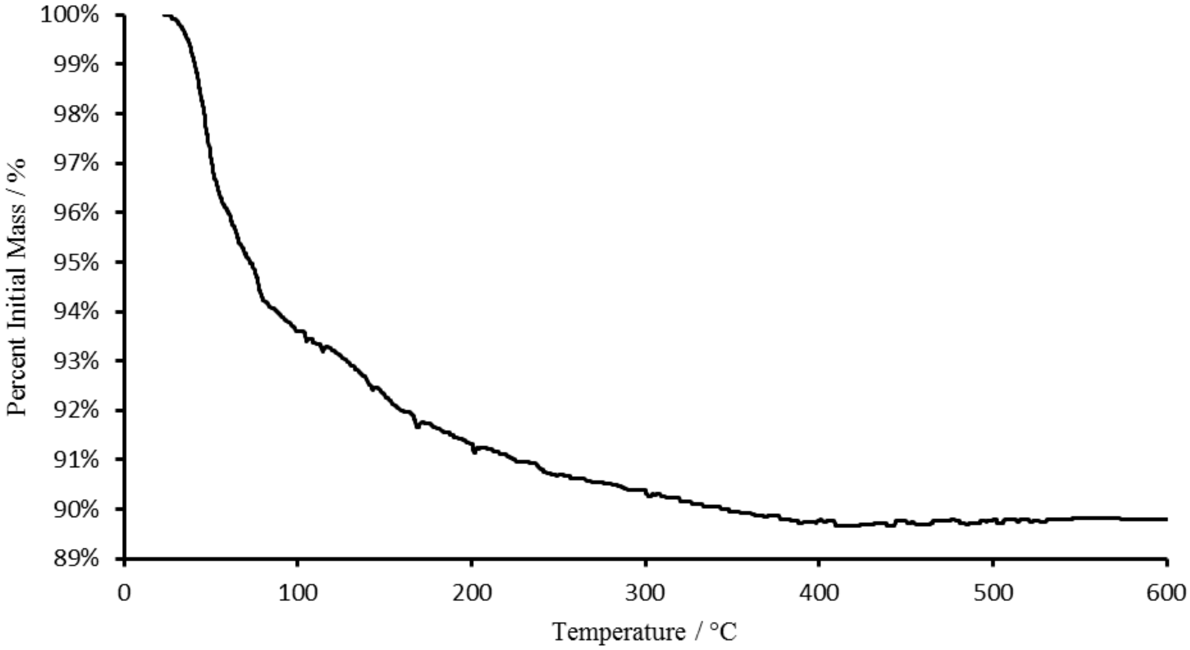

Fig. S2 Thermogravimetric analysis of KH-**1**. The weight loss observed (10.3%) is attributed to waters of hydration and corresponds to 34 water molecules.

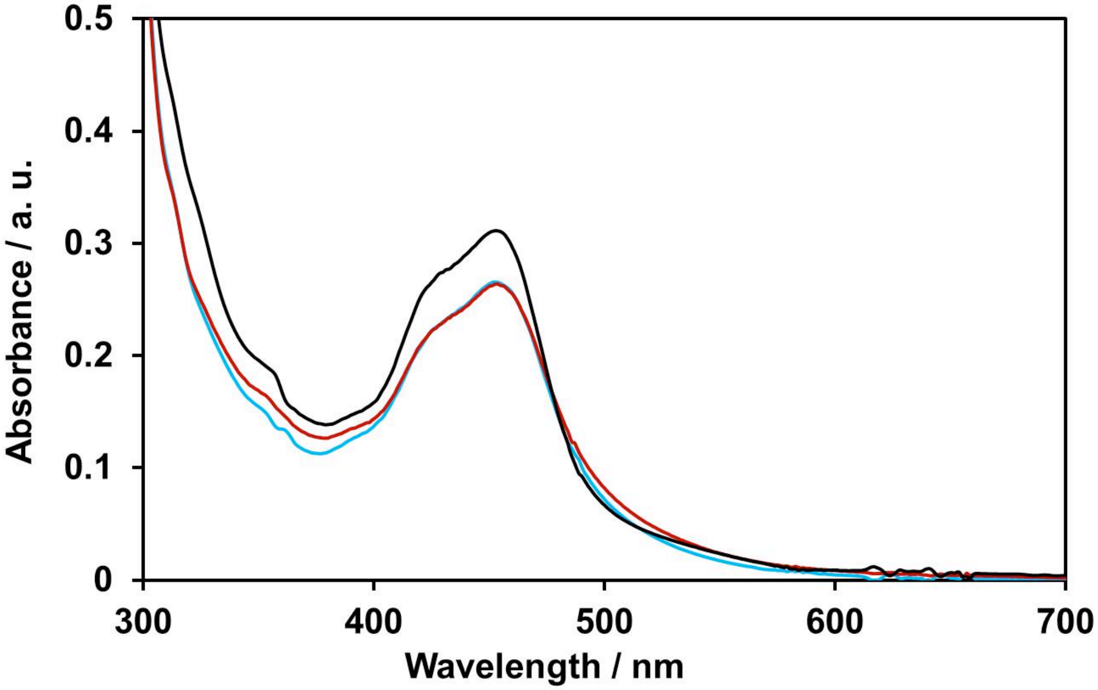

Fig. S3 UV-vis spectra of 40-fold diluted solution of 1 mM $[Ru(bpy)_3]^{2+}$ and 5.0 mM $Na_2S_2O_8$ in 80 mM borate buffer before the photodriven catalytic water oxidation reaction (black curve) and after this reaction (after irradiation) in the absence (blue curve) and presence (red curve) of 2 μM KH-**1**.

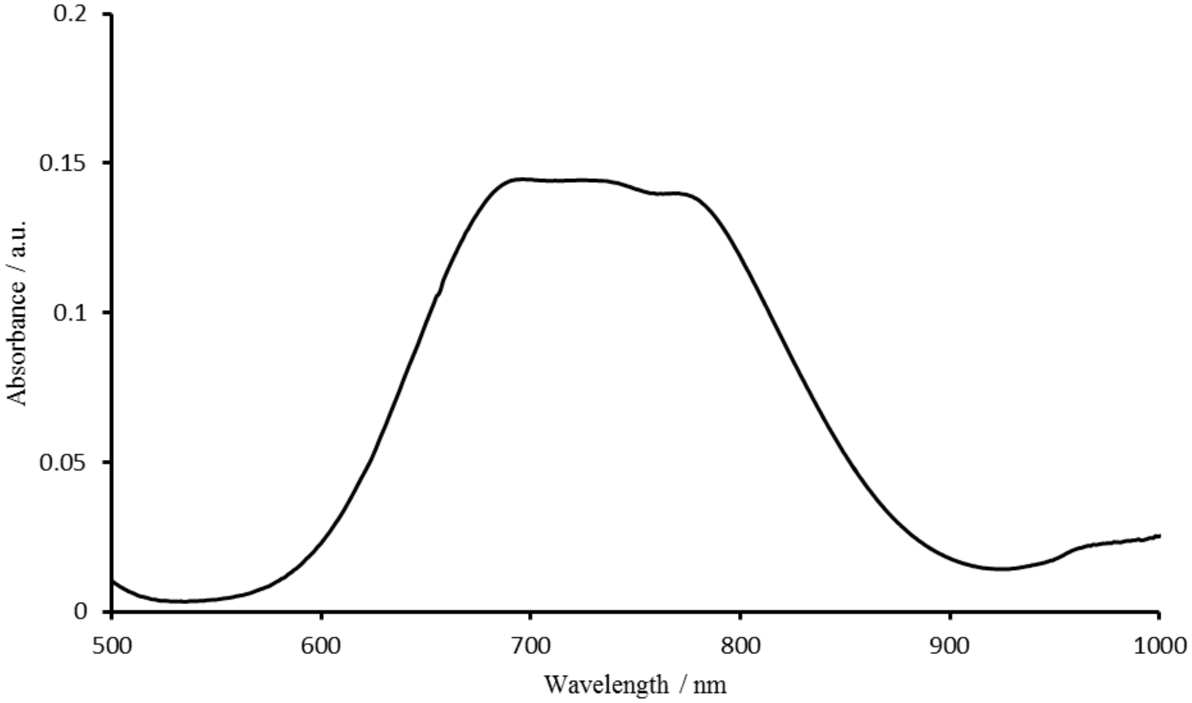

Fig. S4 UV-visible spectrum of 6 mM KH-**1** in 80 mM pH 8 sodium borate buffer.

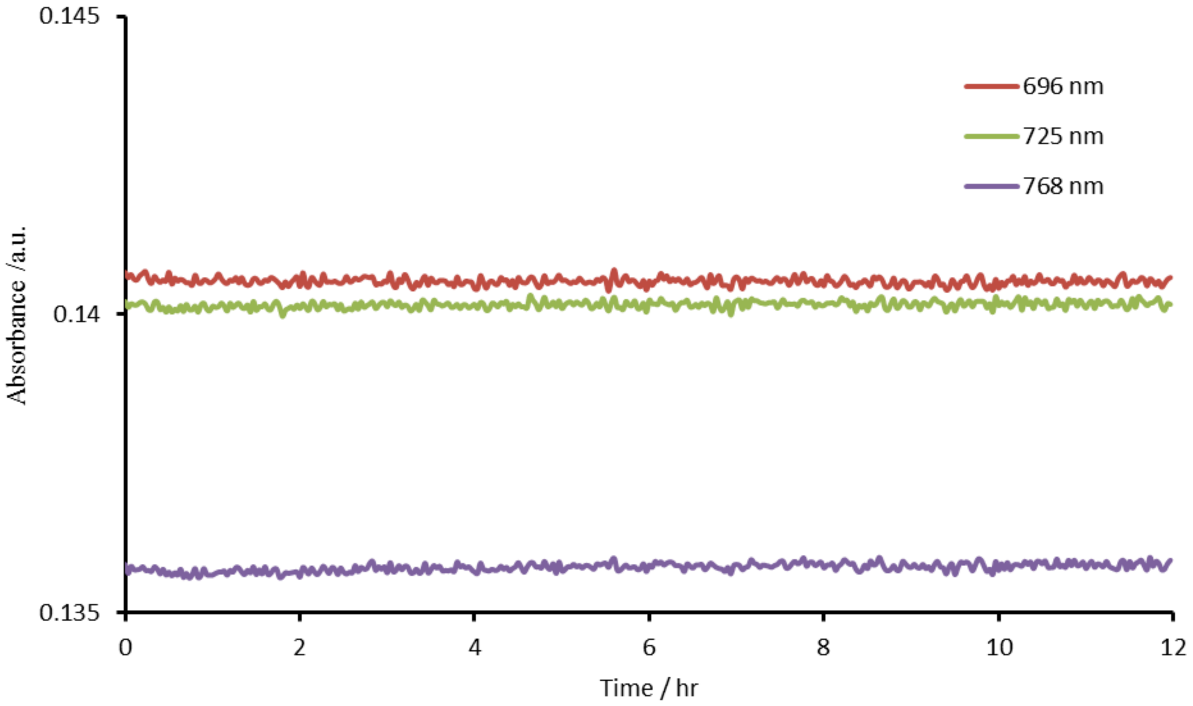

Fig. S5 Kinetic traces of the local maxima of KH-**1** in the UV-visible spectrum of 6 mM KH-**1** in 80 mM pH 8 sodium borate buffer, showing no change in the spectrum upon aging the solution overnight.

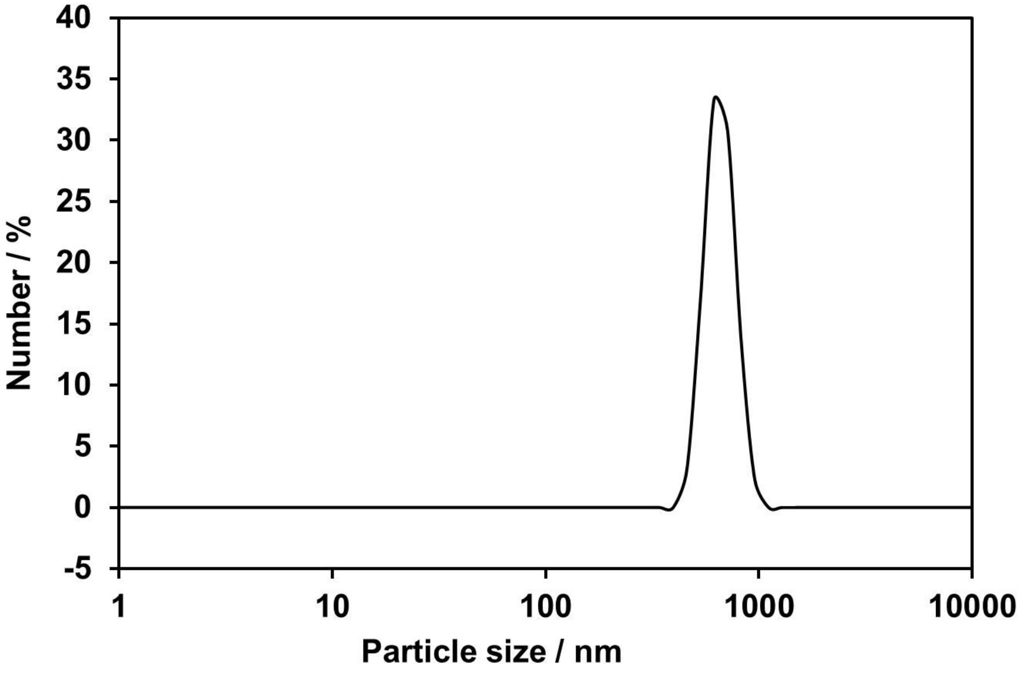

Fig. S6 Particle size distribution measured by DLS in a solution of 0.5 μM KH-**1**, 1 mM $[Ru(bpy)_3]Cl_2$ and 5 mM $Na_2S_2O_8$ in 80 mM pH 8.0 sodium borate buffer.

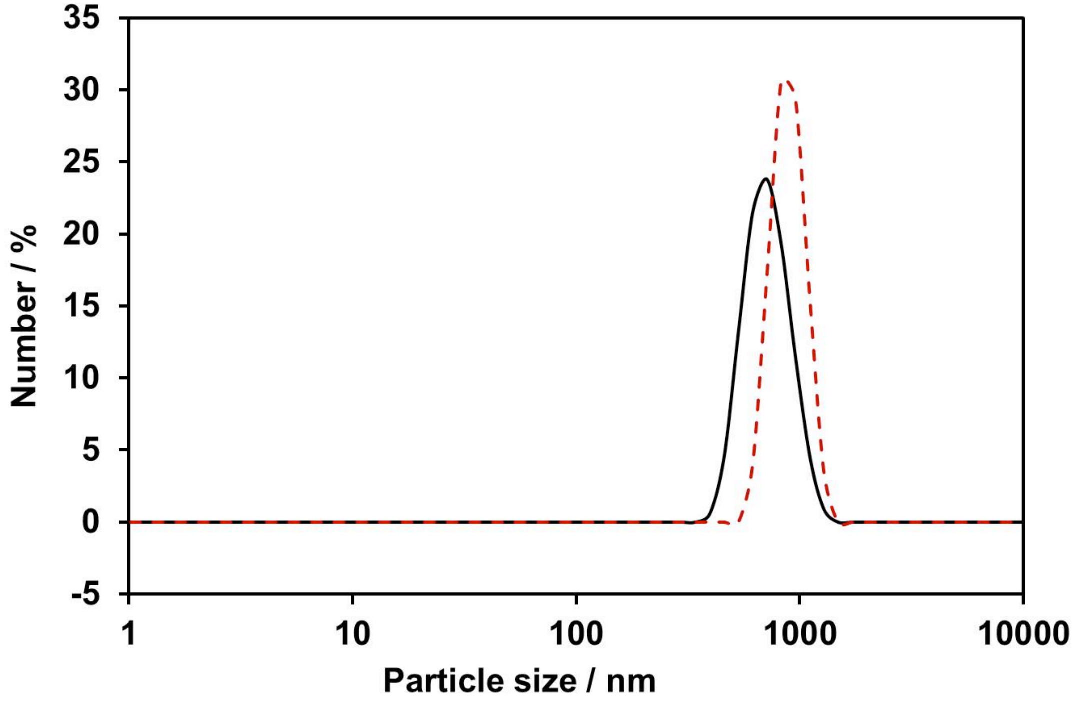

Fig. S7 Particle size distribution measured by DLS in a solution of 2 µM KH-**1**, 1 mM $[Ru(bpy)_3]Cl_2$ and 5 mM $Na_2S_2O_8$ in 80 mM pH 8.0 sodium borate buffer before (red dotted line) and after (black solid line) photoirradiation for 11 min (455 nm LED light, 17 mW).

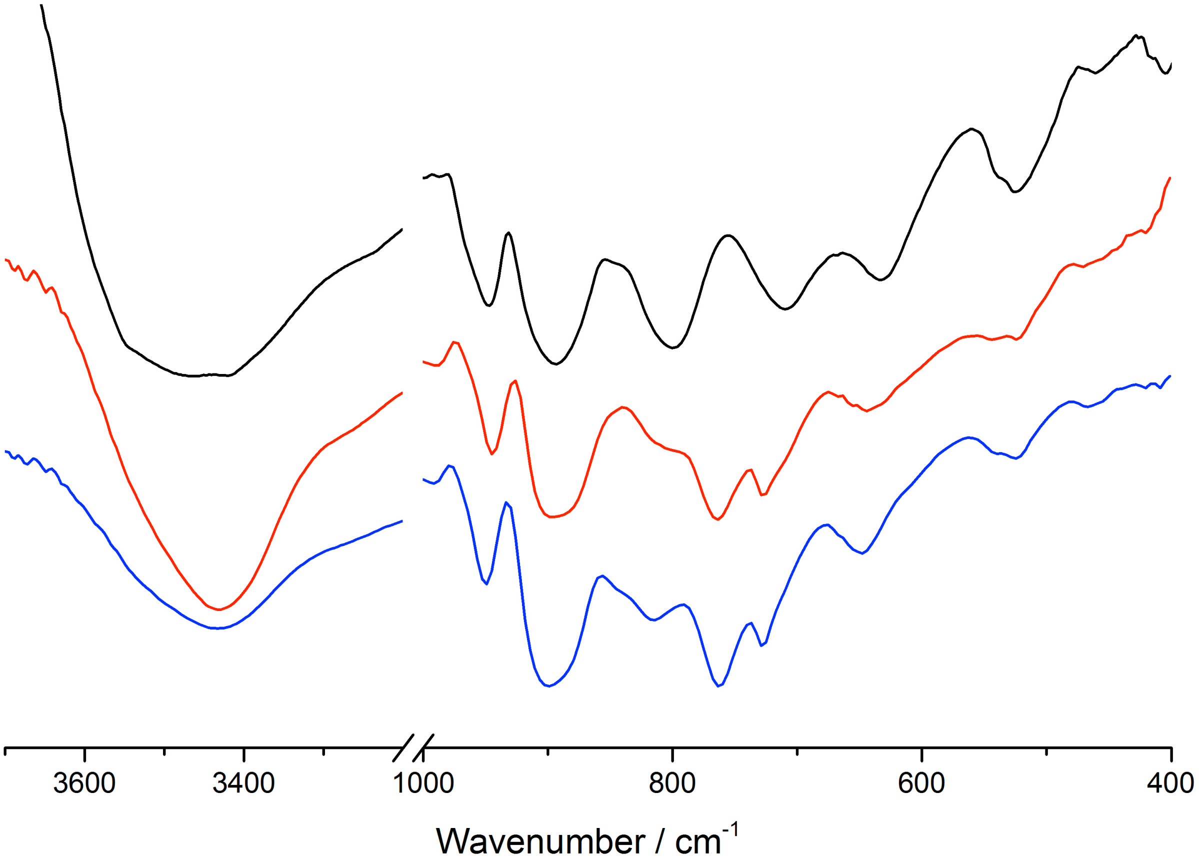

Fig. S8 Infrared spectra of KH-**1**. Black: spectrum of the freshly prepared and purified KH-**1**. Red: precipitate obtained from mixing $[Ru(bpy)_3]^{2+}$ and KH-**1** solutions (the peaks are a simple superposition of the spectra of each compound). Blue: precipitate isolated from a post reaction solution. The spectra before and after water oxidation (irradiation for 100 minutes, TON ca. 40) show no changes indicative of structural rearrangement or metal oxide formation.

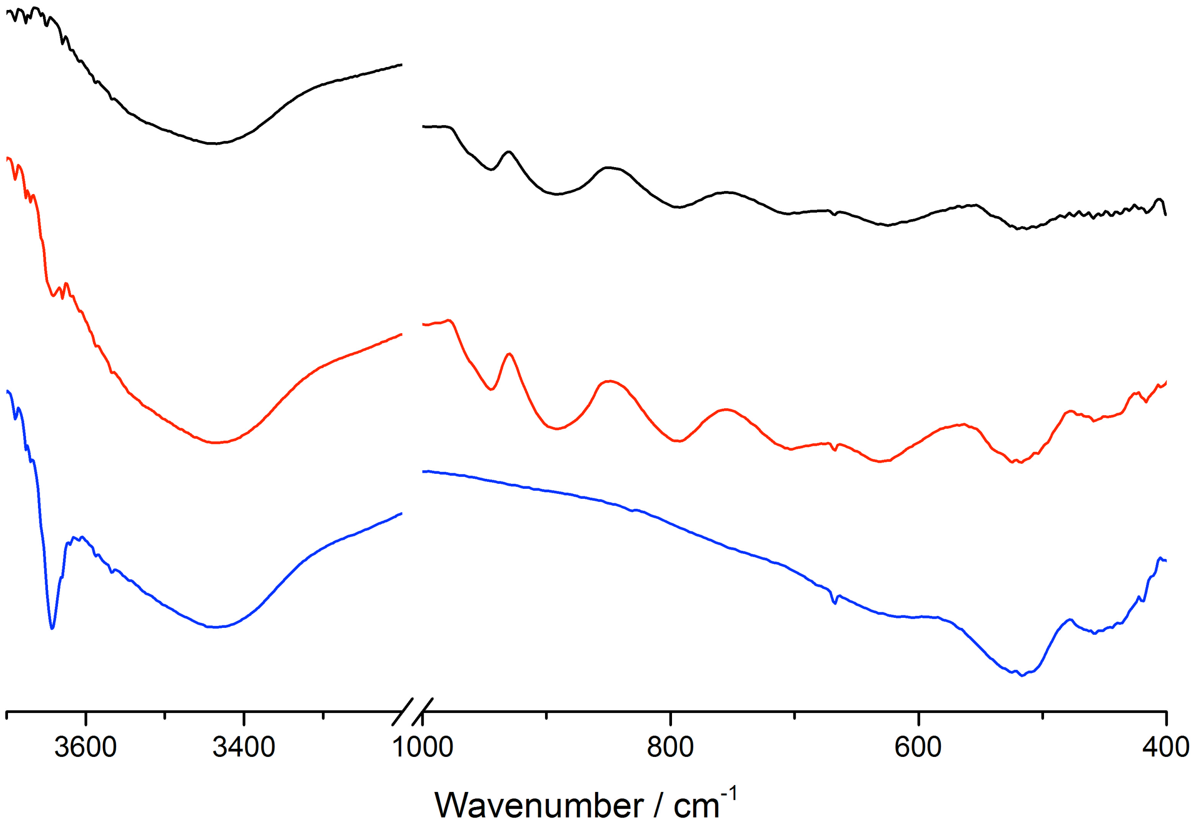

Fig. S9 Infrared spectra of KH-**1** and nickel hydroxide. Black: spectrum of KH-**1**. Red: KH-**1** doped with ~10% nickel hydroxide. Blue: nickel hydroxide, highlighting the characteristic peaks at 525 cm^{-1} and 3640 cm^{-1} that would be visible if KH-**1** decomposes to nickel hydroxide particles under catalytic conditions.

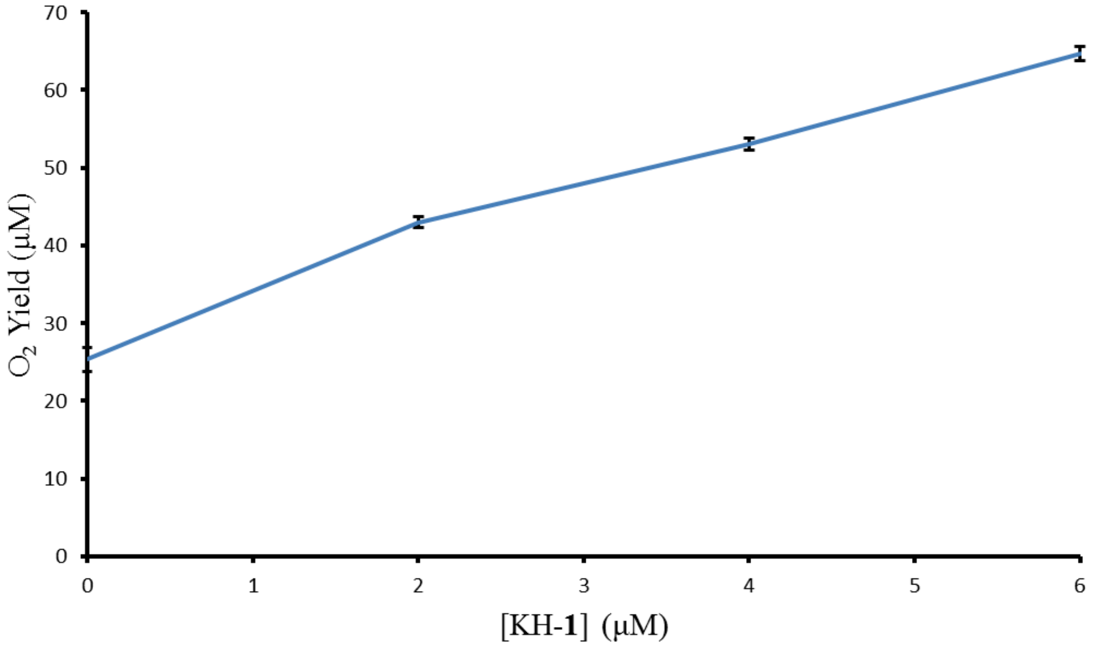

Fig. S10 Fast-mixing O_2 yield vs. KH-**1** concentration in the dark water oxidation reactions measured with a FOXY-R probe using sacrificial oxidant $[Ru(bpy)_3]^{3+}$. Each point represents the average of three consecutive shots, with error bars showing the range of measured values. Conditions: 1 mM $[Ru(bpy)_3]^{3+}$, 80 mM sodium borate buffer at pH 8.0.

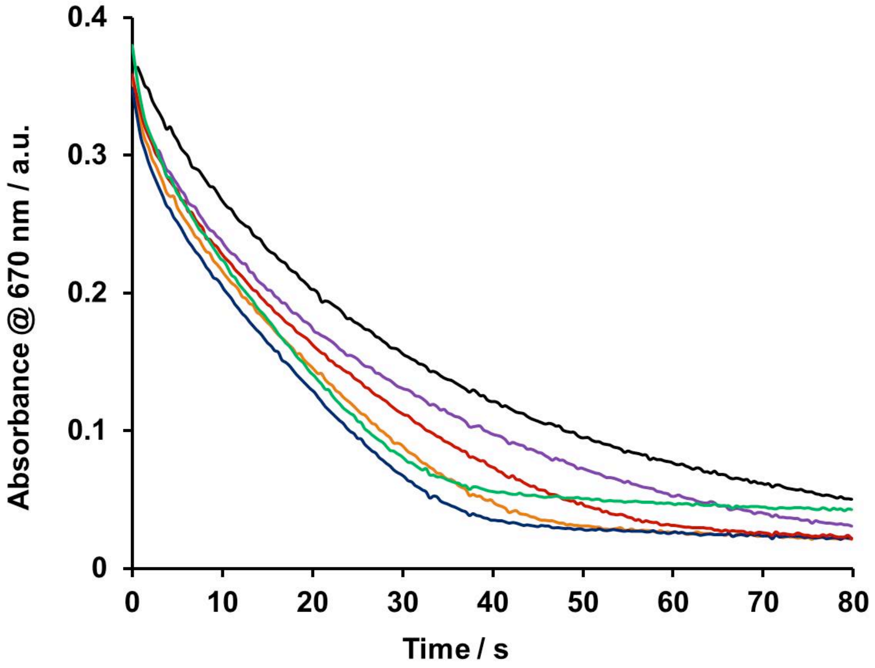

Fig. S11 Kinetics of $[Ru(bpy)_3]^{3+}$ self-decomposition (black) and catalytic reduction with 1 μM (purple), 2 μM (red), 3 μM (orange), 4 μM (blue), 5 μM (green) KH-**1.** Conditions: 1.0 mM $[Ru(bpy)_3]^{3+}$, 80 mM sodium borate buffer with initial pH 8.0, in the dark.

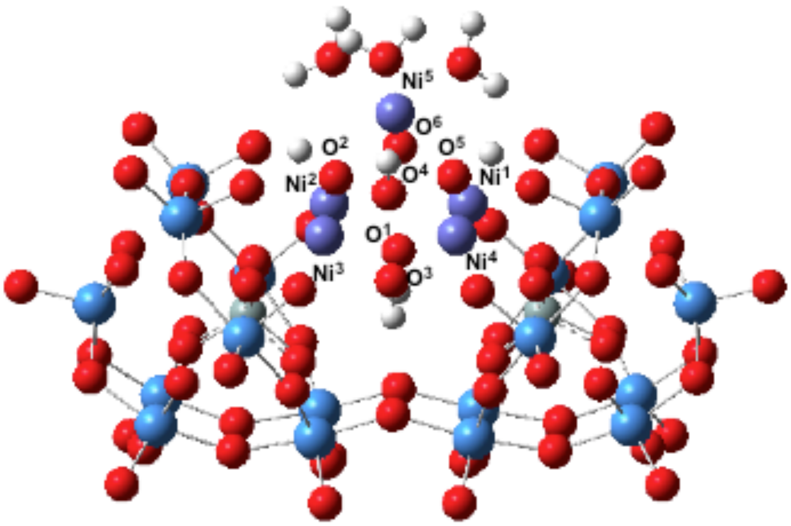

Fig. S12 Notation of atoms in the calculated structure of KH-**1**.